frontiers in
ENERGY RESEARCH

REVIEW ARTICLE
published: 27 June 2014
doi: 10.3389/fenrg.2014.00025

Recent advances in inorganic solid electrolytes for lithium batteries

Can Cao[1,2], Zhuo-Bin Li[2], Xiao-Liang Wang[2†], Xin-Bing Zhao[1]* and Wei-Qiang Han[1,2,3]*

[1] *Department of Materials Science and Engineering, Zhejiang University, Hangzhou, China*
[2] *Ningbo Institute of Materials Technology and Engineering, Chinese Academy of Sciences, Ningbo, China*
[3] *School of Physical Science and Technology, ShanghaiTech University, Shanghai, China*

Edited by:
Mariusz Walkowiak, Institute of Non-Ferrous Metals, Poland

Reviewed by:
Lei Li, Shanghai Jiao Tong University, China
Jie Shu, Ningbo University, China
Xiao-Guang Sun, Oak Ridge National Laboratory, USA

***Correspondence:**
Xin-Bing Zhao, Department of Materials Science and Engineering, Zhejiang University, 38#, Zheda Road, Hangzhou, Zhejiang Province, China
e-mail: zhaoxb@zju.edu.cn;
Wei-Qiang Han, 1219#, Zhongguan Road, Ningbo, Zhejiang Province, China
e-mail: hanweiqiang@nimte.ac.cn

[†]***Present address:***
Xiao-Liang Wang, Seeo, Inc., 3906 Trust Way, Hayward, CA 94545, USA

The review presents an overview of the recent advances in inorganic solid lithium ion conductors, which are of great interest as solid electrolytes in all-solid-state lithium batteries. It is focused on two major categories: crystalline electrolytes and glass-based electrolytes. Important systems such as thio-LISICON $Li_{10}SnP_2S_{12}$, garnet $Li_7La_3Zr_2O_{12}$, perovskite $Li_{3x}La_{(2/3)-x}TiO_3$, NASICON $Li_{1.3}Al_{0.3}Ti_{1.7}(PO_4)_3$, and glass–ceramic $xLi_2S{\cdot}(1-x)P_2S_5$ and their progress are described in great detail. Meanwhile, the review discusses different ongoing strategies on enhancing conductivity, optimizing electrolyte/electrode interface, and improving cell performance.

Keywords: all-solid-state, lithium batteries, inorganic electrolytes, ion conductivity, interface

INTRODUCTION

Lithium batteries are being scrutinized as the most promising electrical energy storage for electric vehicles (EVs), which hold great promise in resolving the jeopardy on future transportation. On the other hand, they have not yet been able to meet automobiles' stringent requirement on high energy density, long cycle life, excellent safety, and wide operating temperature range (Goodenough and Kim, 2009; Kotobuki, 2012).

In order to get lithium batteries ready for their large-scale implementation in EVs, researchers extensively look at all aspects in a cell that would leapfrog the cell performance (e.g., novel electrolytes, high energy-density, and stable electrode materials, high-performance conductive additives/binders/current collectors, and efficient packaging). Among these approaches, the electrolyte holds the key to the success of EV batteries. The state-of-the-art electrolytes mainly consist of lithium salts and organic solvents. Therefore, they cause irreversible capacity losses resulted from the formation of stable solid electrolyte interphase (SEI), hinder the increase in cycle life, limit the temperature window, and, not to mention, pose severe safety concerns on lithium batteries.

In this respect, the replacement of currently used organic liquid electrolytes with inorganic solid electrolytes (SEs) is very appealing. For one thing, inorganic SEs are solid materials. Thus, they can address the above-mentioned concerns on capacity losses, cycle life, operation temperatures, safety and reliability (Hayashi et al., 2012; Sahu et al., 2014). In addition, they present advantages such as the simplicity of design, absence of leakage and pollution, better resistance to shocks and vibrations compared to organic liquid electrolytes (Thangadurai and Weppner, 2006b; Knauth, 2009; Fergus, 2010). For another thing, most of inorganic SEs are single ion conductors. Lithium single ion conductors can have a lithium transference number of unity. As a result, there is no concentration gradient inside the cell while it is operating. This is very beneficial to the lowering of cell overpotential (Quartarone and Mustarelli, 2011).

Also stemming from these two prominent features, great challenges remain for achieving high-performance SEs. One of them is how to create favorable solid–solid interface between electrode and electrolyte (Ohta et al., 2006, 2007; Sakuda et al., 2011). Another one is how to obtain high ionic conductivity at room temperature, e.g., 10^{-3} S cm^{-1}.

In this review, the advantages, as well as efficient ways to addressing the aforementioned grant challenges, are discussed. The first part is about crystalline electrolytes, including LISICON and thio-LISICON-type, Garnet-type, Perovskite-type, and NASICON-type lithium ion conductors. The second part is about glass-based electrolytes, including glassy and glass-ceramic systems made of oxides and sulfides. **Table 1** lists important materials and their conductivities and **Figure 1** shows Arrhenius plots for ionic conductivities of some selected SEs.

Table 1 | Conductivity of inorganic SEs for all-solid-state lithium batteries.

Type	Example	Conductivity (S cm^{-1})		Reference
		RT*	HT*	
Crystal (LISICON)	$Li_{14}ZnGe_4O_{16}$	1.0×10^{-7}	1.3×10^{-1} (300°C)	Hong (1978)
Crystal (thio-LISICON)	$Li_{10}GeP_2S_{12}$	1.2×10^{-2}	1.3×10^{-1} (100°C)	Kamaya et al. (2011)
Crystal (thio-LISICON)	$Li_{10}SnP_2S_{12}$	4×10^{-3}	1.0×10^{-2} (60°C)	Bron et al. (2013)
Crystal (garnet)	$Li_{6.5}La_3Nb_{1.25}Y_{0.75}O_{12}$	2.7×10^{-4}	1.2×10^{-3} (75°C)	Narayanan et al. (2012)
Crystal (garnet)	$Li_7La_3Zr_2O_{12}$	2.1×10^{-4}	7.1×10^{-4} (75°C)	Dumon et al. (2013)
Crystal (garnet)	$Li_{6.75}La_3Zr_{1.75}Ta_{0.25}O_{12}$	8.7×10^{-4}	3.9×10^{-3} (100°C)	Allen et al. (2012)
Crystal (perovskite)	$Li_{3x}La_{(2/3)-x}TiO_3$ ($x = 0.11$)	1.0×10^{-3}	5.6×10^{-3} (100°C)	Stramare et al. (2003)
Crystal (NASICON)	$Li_{1+x}Al_xTi_{2-x}(PO_4)_3$ ($x = 0.3$)	7×10^{-4}	1.1×10^{-2} (100°C)	Aono et al. (1990)
Glass	$50Li_2O$-50 ($0.5SeO_2 - 0.5B_2O_3$)	8×10^{-7}	–	Lee et al. (2002)
Glass	$50Li_2S$-$17P_2S_5 - 33LiBH_4$	1.6×10^{-3}	6.4×10^{-3} (100°C)	Yamauchi et al. (2013)
Glass–ceramic	$Li_{1.6}Al_{0.6}Ge_{1.4}(PO_4)_3$	4.0×10^{-4}	1.2×10^{-3} (50°C)	Fu (1997a)
Glass–ceramic	$70Li_2S{\cdot}30P_2S_5$	1.7×10^{-2}	8×10^{-2} (100°C)	Seino et al. (2014)

RT, room temperature; HT*, high-temperature.*

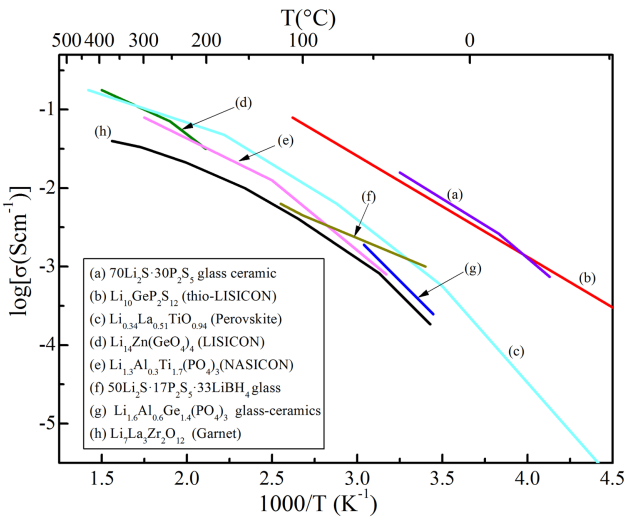

FIGURE 1 | Arrhenius plots for ionic conductivities of selected SEs.

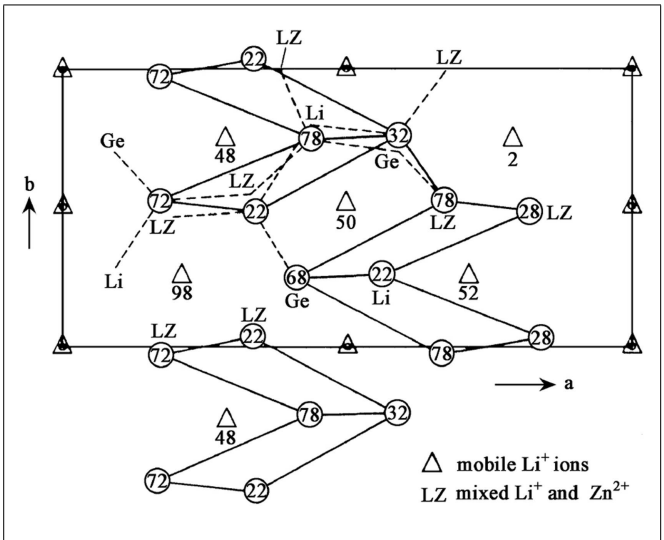

FIGURE 2 | Projection of the LISICON structure on the a-b plane. Reproduced with permission of Hong (1978).

CRYSTALLINE INORGANIC ELECTROLYTES

LISICON AND THIO-LISICON-TYPE ELECTROLYTES

LISICON-type SEs possess relatively low conductivity at room temperature (~10^{-7} S cm^{-1}) and $Li_{14}ZnGe_4O_{16}$ is its typical representative, which was first described by Hong (1978). Its one member of $Li_{2+2x}Zn_{1-x}GeO_4$ system and can be viewed as a Li_4GeO_4–Zn_2GeO_4 solid solution. **Figure 2** shows the projection of the LISICON structure on the a-b plane, whose framework is related to the γ-Li_3PO_4 crystal structure. $Li_{11}ZnGe_4O_{16}$ forms a three-dimensional (3D) skeleton structure and lithium ions in the skeleton distribute in two sites: 4c and 8d sites. These sites are occupied by four and seven Li^+ ions, respectively. The three remaining Li^+ ions are located in 4c and 4a interstitial sites and their temperature coefficients are abnormally high, indicating that they can be mobile. Each 4a site is connected to two 4c sites and vice versa. The bottlenecks to Li^+ transport between these sites are parallelograms, which have a tilt angle with the a-b plane. On the basis of calculation, the average size of the bottlenecks (4.38 Å) is bigger than the minimum size required for Li^+ transport ($2r_{Li} + 2r_o = 4.0$ Å), which promotes Li^+ movement (Zheng et al., 2003).

Although the ionic conductivity of $Li_{14}ZnGe_4O_{16}$ is as high as 0.125 S cm^{-1} at 300°C, it is only 10^{-7} S cm^{-1} at room temperature. This is explained by trapping of the mobile Li^+ ions by the immobile sublattice at lower temperatures via the formation of defect complexes (Robertson et al., 1997). Furthermore, $Li_{14}ZnGe_4O_{16}$ is highly reactive with Li-metal and atmospheric CO_2 and the conductivity decreases with time (Thangadurai and Weppner, 2006b).

Recent efforts to improve the ionic conductivity of LISICON-type SEs focus on the replacement of oxide by sulfur in the framework (**Figure 3**). These sulfide SEs are referred to as thio-LISICON, which was introduced by Kanno et al. (2000).

Material design of inorganic SEs are based on certain structural criteria: (i) mobile ions should have conduction pathways large enough in the lattice, (ii) there should be a disordered mobile ion sublattice, and (iii) highly polarizable mobile ions and anion sublattices are preferable (Kanno and Murayama, 2001). The ionic conduction properties are strongly dominated by the size and polarizability of constituent ions, or interstitial vacancy character caused by the substitutions.

Since the radius of S^{2-} is higher than O^{2-}, this substitution can significantly enlarge the size of Li^+ transport bottlenecks. Besides, S^{2-} has better polarization capability than O^{2-}, thus weakens the interaction between skeleton and Li^+ ions. Therefore, compared with LISICON systems, thio-LISICON materials can achieve really high ionic conductivity (over 10^{-4} S cm^{-1} at room temperature). Thio-LISICON SEs also have advantages, such as easy reduction of grain-boundary resistance by conventional cold-press of electrolyte powers and preferable application to all-solid-state batteries due to its mechanical property (Tatsumisago et al., 2013).

A series of thio-LISICON were firstly synthesized and $Li_{3.25}Ge_{0.25}P_{0.75}S_4$ showed a high conductivity of 2.2×10^{-3} S cm^{-1} at room temperature, negligible electronic conductivity, high electrochemical stability, and no phase transition up to 500°C (Kanno and Murayama, 2001). Most recently, a very high conductivity of 12 m S cm^{-1} (27°C) was achieved by $Li_{10}GeP_2S_{12}$. Its crystal structure was different from typical thio-LISICON structures. As shown in **Figure 4A**, it had a 3D framework structure consisting of $(Ge_{0.5}P_{0.5})S_4$ tetrahedra, PS_4 tetrahedra, LiS_4 tetrahedra, and LiS_6 octahedra. The high ionic conductivity benefited from the 3D diffusion pathways both along *c* axis and in a-b plane (Kamaya et al., 2011).

Furthermore, Bron et al. (2013) reported the synthesis of $Li_{10}SnP_2S_{12}$ by replacing Ge with Sn, whose total conductivity reached 4 m S cm^{-1} at room temperature. All-solid-state battery with $Li_{10}GeP_2S_{12}$ (cathode: $LiCoO_2$; anode: in metal) exhibited a discharge capacity of over 120 mA g^{-1} and an excellent coulombic efficiency of about 100% after the second cycle as well as a high decomposition potential of over 5 V (**Figure 4B**).

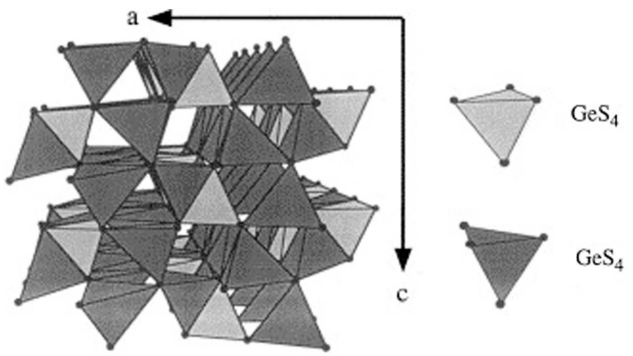

FIGURE 3 | Structure of Li_4GeS_4-a parent structure of the new thio-LISICON family. Reproduced with permission of Kanno et al. (2000).

GARNET-TYPE ELECTROLYTES

Garnet-type lithium single ion conductors have a general formula of $Li_5La_3M_2O_{12}$ (M = Ta, Nb). They were firstly reported by Thangadurai and Weppner (2005a) and recently have been intensively studied as SEs for all-solid-state lithium batteries. They have high ionic conductivity and excellent chemical stability in contact with lithium metal.

Figure 5 shows the crystal structure of $Li_5La_3M_2O_{12}$. La and M occupy eight- and six-coordinated sites, respectively,

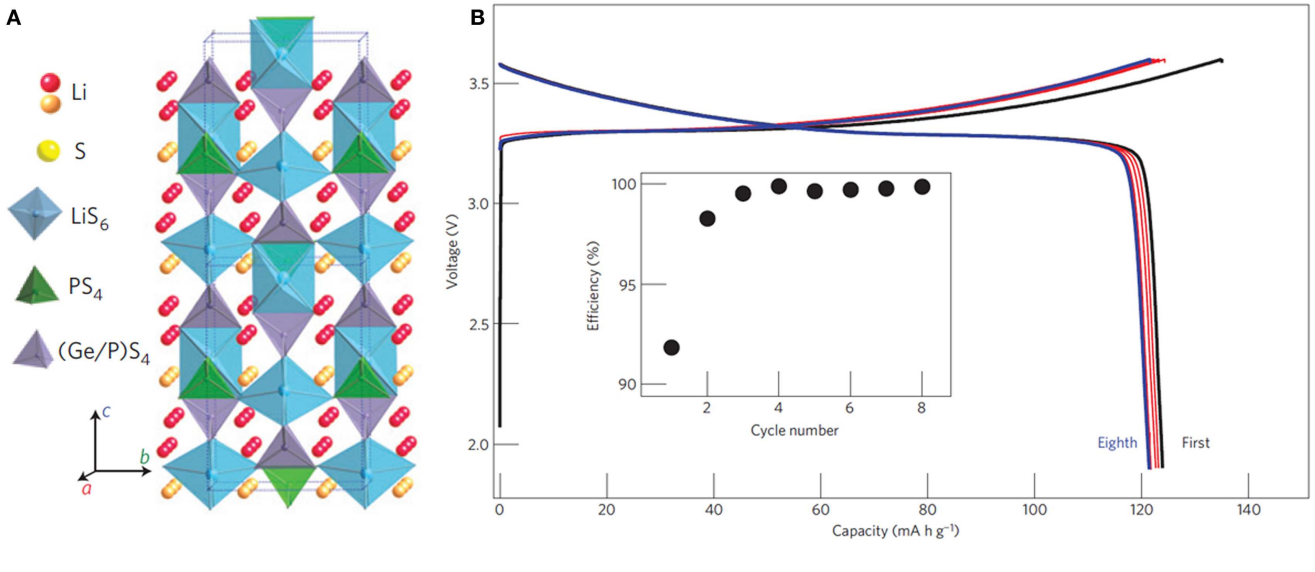

FIGURE 4 | (A) Crystal structure of $Li_{10}GeP_2S_{12}$. **(B)** Charge–discharge curves of an all-solid-state battery with this SE. Reproduced with permission of Kamaya et al. (2011).

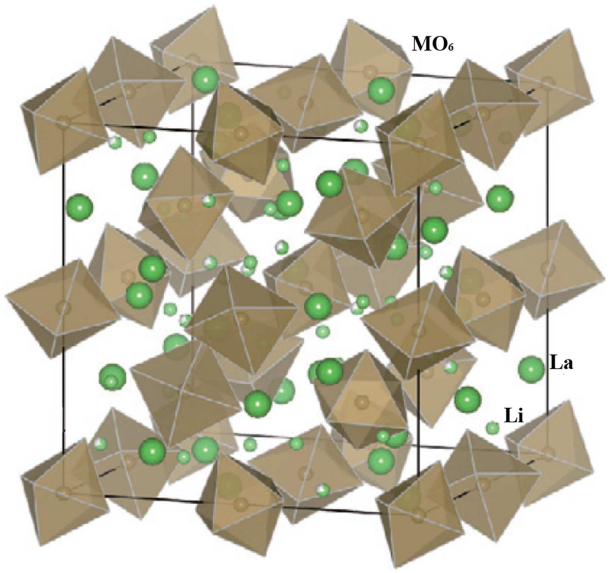

FIGURE 5 | Crystal structure of parent garnet-like $Li_5La_3M_2O_{12}$. Reproduced with permission of Takada (2009).

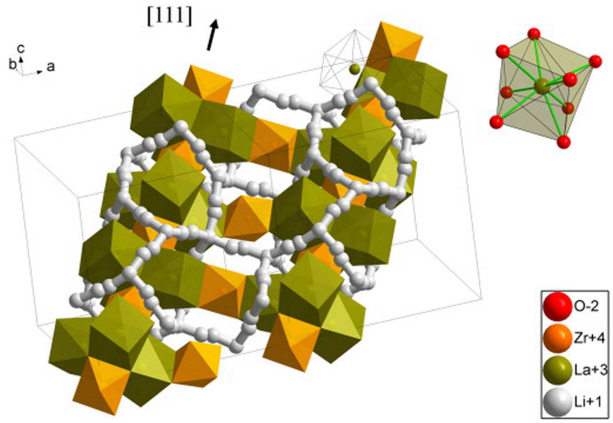

FIGURE 6 | Crystallographic structure of cubic LLZO. Reproduced with permission of Dumon et al. (2013).

and Li occupies octahedral sites. The MO_6 octahedra are surrounded by six lithium ions and two Li^+ vacancies in the parent $Li_5La_3M_2O_{12}$ structure. Therefore, the structure facilitates lithium ion conduction (Thangadurai and Weppner, 2005b).

Among the materials investigated, $Li_6BaLa_2Ta_2O_{12}$ exhibited a high ionic conductivity of 4×10^{-5} S cm^{-1} at 22°C with an activation energy of 38.5 kJ mol^{-1}. It had low grain-boundary resistance, which meant that the total and bulk conductivities were nearly identical (Thangadurai and Weppner, 2005b).

Conductivity can be further improved through partially substitution of Y or In at the M site in $Li_5La_3M_2O_{12}$. For example, $Li_{5.5}La_3Nb_{1.75}In_{0.25}O_{12}$ showed an enhanced conductivity (1.8×10^{-4} S cm^{-1} at 50°C) with low activation energy of 49.1 kJ mol^{-1} (Thangadurai and Weppner, 2006a). High conductivity of 2.7×10^{-4} S cm^{-1} at 25°C was obtained for $Li_{5+2x}La_3Nb_{2-x}Y_xO_{12}$ with $x = 0.75$ (Narayanan et al., 2012). The high Li^+ conductivity resulted from short Li^+–Li^+ distances in the edge-sharing LiO_6 octahedra and a high concentration of Li on the octahedral sites.

Recently, garnet-type $Li_7La_3Zr_2O_{12}$ (LLZO) has attracted much attention since firstly reported (Murugan et al., 2007). In the structure, La is located at the center of a dodecahedron with eight coordinated oxygen atoms while Zr is at the center of an octahedron with six-coordinated oxygen atoms (**Figure 6**). The lithium ions could migrate within the garnet lattice framework with a 3D conduction mechanism (Dumon et al., 2013).

LLZO undergoes a phase change from tetragonal to cubic structure as the sintering temperature increases, which belong to the space group Iad and $I4_1A/cd$, respectively. Conductivity of the cubic phase (10^{-4} S cm^{-1}, room temperature) is about two orders of magnitude higher than that of the tetragonal phase (Kokal et al., 2011; Tietz et al., 2013).

Therefore, the challenge has been to stabilize the cubic phase, which can be achieved by doping. Geiger et al. (2011) firstly suggested the important role Al could play to stabilize the cubic phase relative to the tetragonal phase. Then Düvel et al. (2012) described in depth the effects of Al incorporation on both structural and dynamic properties of LLZO. It was suggested that at low Al concentrations Al^{3+} ions acted as an aliovalent dopant by replacing three Li^+ ions. However, with increasing Al content, La^{3+} and Zr^{4+} ions were progressively replaced by Al ions. The substitution of La^{3+} and Zr^{4+} with Al^{3+} ions stabilized the cubic phase and greatly affected the corresponding Li ion dynamics. Similar stabilization of the cubic phase was observed with Ga and Ta substitution. Allen et al. (2012) recently reported $Li_{6.75}La_3Zr_{1.75}Ta_{0.25}O_{12}$ cubic garnet with relatively high total Li^+ conductivity (8.7×10^{-4} S cm^{-1} at 25°C).

Owing to its high ionic conductivity, excellent stability with Li and wide electrochemical voltage window (Ishiguro et al., 2013; Jin and McGinn, 2013b), LLZO has been successfully used to fabricate all-solid-state lithium batteries. Jin and McGinn (2013a) reported a $Cu_{0.1}V_2O_5$/LLZO/Li all-solid-state battery, which exhibited an initial discharging capacity of 93 mA h g^{-1} at 10 μA cm^{-2} (at 50°C). A full cell consisting of a $LiCoO_2$ cathode, a $Li_{6.75}La_3Zr_{1.75}Nb_{0.25}O_{12}$ electrolyte and Li-metal anode exhibited stable cycle performance (**Figure 7**). Its discharge capacities were 129 mA h g^{-1} at the 1st cycle and 127 mA h g^{-1} at the 100th cycle, respectively (Ohta et al., 2012).

PEROVSKITE-TYPE ELECTROLYTES

The lithium–lanthanum–titanates, $Li_{3x}La_{(2/3)-x}\square_{(1/3)-2x}TiO_3$ (LLTO, $0 < x < 0.16$), with the perovskite structure (ABO_3), are characteristic of high bulk conductivity, of the order of 10^{-3} S cm^{-1} at room temperature (Bohnke, 2008).

LLTO consists of a mixture of phases, i.e., a high-temperature phase with cubic *Pm3m* symmetry (α-LLTO) and a lower temperature β-LLTO phase having tetragonal *P4/mmm* symmetry. **Figure 8** shows the crystal structure of LLTO. The A site cations, which were Li^+ and La^{3+} in the cubic α-LLTO phase, were randomly distributed, while the A sites of the ordered β-LLTO had

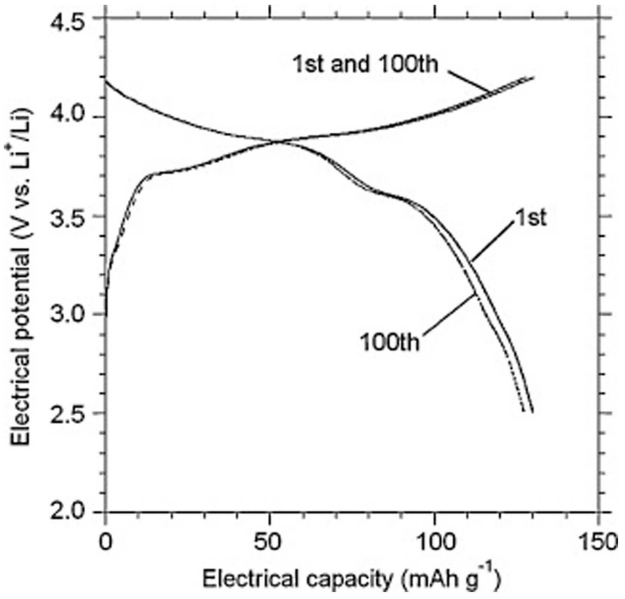

FIGURE 7 | Charge-discharge curves for the $LiCoO_2/Li_{6.75}La_3Zr_{1.75}Nb_{0.25}O_{12}$/Li cell. Reproduced with permission of Ohta et al. (2012).

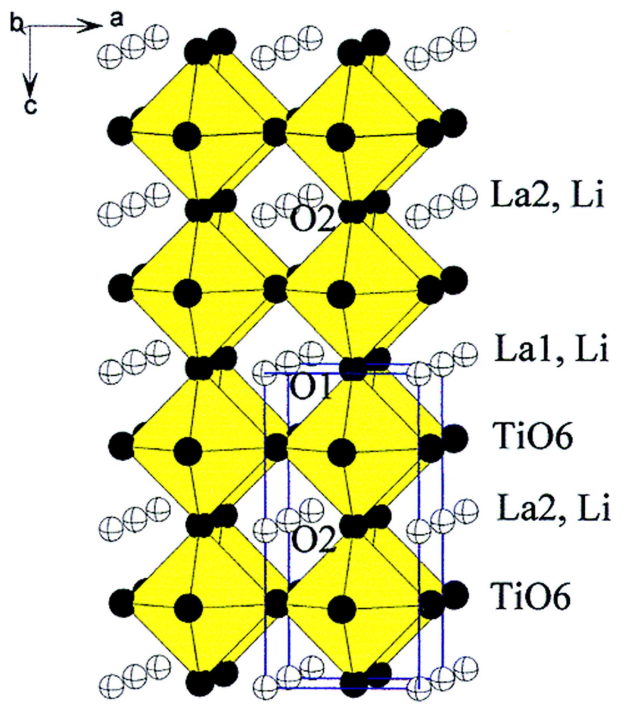

FIGURE 8 | Crystal structure of tetragonal LLTO. Reproduced with permission of Stramare et al. (2003).

a doubled perovskite structure, with an alternating arrangement of La-rich and Li-vacancy-rich layers along the *c* axis (Gao et al., 2013; Teranishi et al., 2013). It is believed that the conductivity of LLTO electrolytes is mainly governed by two factors: bottleneck size and site percolation. The crystal structure of tetragonal LLTO explains the high Li^+ conductivity by the large concentration of A site vacancies, allowing motion of lithium ions by a vacancy mechanism and through square planar bottleneck between A sites, formed by four O^{2-} ions between two neighboring A sites (Alonso et al., 2000).

LLTO-based SEs have many advantages, such as lithium single ion conductors, negligible electronic conductivity, high electrochemical stability (>8 V), stability in dry and hydrated atmospheres, and stability over a wide temperature range from 4 K to 1600 K (Bohnke, 2008). However, there are two major challenges for LLTO electrolytes, i.e., relatively low grain-boundary conductivity ($<10^{-5}$ S cm^{-1}) and the instability against Li metal anode (Ban and Choi, 2001).

Thus, it is of utmost importance to increase the grain-boundary conductivity of LLTO electrolytes. It has been reported that the introduction of silica (Mei et al., 2010) and LLZO (Chen et al., 2012, 2013) could modify the grain-boundary layer of LLTO, and the total ionic conductivity could be over 1×10^{-4} and 1.2×10^{-4} S cm^{-1} at room temperature, respectively. A high conductivity was also achieved by doping Al (Morata-Orrantia et al., 2003) or Nb (Teranishi et al., 2013), whereas the addition of Ag (Abhilash et al., 2013) led to a decrease in conductivity. The replacement of some oxygen with fluorine did not significantly affect the conductivity (Fergus, 2010). Furthermore, effective sintering to decrease grain boundary is important to improve total conductivity (Vidal et al., 2014).

Another issue that lies with LLTO is its instability against Li metal anode. Lithium can be intercalated into LLTO at a potential below about 1.7–1.8 V vs. Li (Chen and Amine, 2001), which causes the reduction of Ti^{4+} to Ti^{3+} and induces high electronic conductivity. Nevertheless, chemical substitutional studies have been undergoing motivated by the discovery of new applications for LLTO compounds in future figurations of lithium ion batteries: as cathode coatings (Qian et al., 2012) or electrolyte separators (Inaguma and Nakashima, 2013). As shown in **Figure 9**, the stable discharge/charge behaviors of a rechargeable lithium/air cell with LLTO separator were confirmed.

NASICON-TYPE ELECTROLYTES

The term NASICON, which stands for Na^+ super ionic conductors, was first given to the solid solution phase $Na_{1+x}Zr_2Si_xP_{3-x}O_{12}$, $x = 2.0$, discovered by Hong (1976). The general formula of NASICON-type SE can be described as $LiA_2^{IV}(PO_4)_3$ (A^{IV} = Ti, Zr, Ge, Hf).

In the structure, AO_6 octahedra are linked by PO_4 tetrahedra to form 3D interconnected channels and two types of interstitial positions (M′ and M″) where mobile cations are distributed, as shown in **Figure 10**. The mobile cations move from one site to another through bottlenecks, the size of which depends on the nature of the skeleton ions and on the carrier concentration in both type of sites (M′ and M″) (Cretin and Fabry, 1999).

Among the $LiA_2^{IV}(PO_4)_3$ NASICONs, the systems with Ti exhibited high Li^+ conductivity (about 10^{-5} S cm^{-1} at room temperature) (Takada, 2009). This could be explained by the ionic radius of Li^+ matching well with the size of skeleton framework, which consists of TiO_6 octahedra. Great efforts have

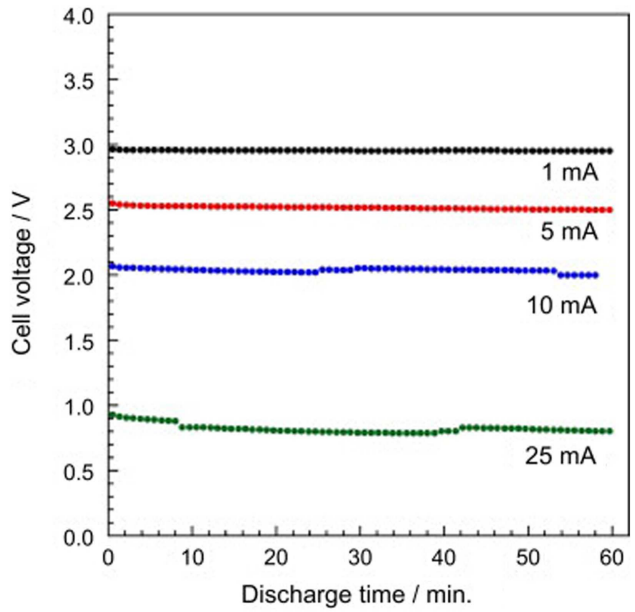

FIGURE 9 | Discharge curve of the lithium-air battery using LLTO as a separator at various currents. Reproduced with permission of Inaguma and Nakashima (2013).

been made for maximizing the ionic conductivity of $LiA_2^{IV}(PO_4)_3$ systems, especially $LiTi_2(PO_4)_3$. An increase in conductivity was observed when Ti^{4+} was partially substituted by Al^{3+} in $Li_{1+x}Al_xTi_{2-x}(PO_4)_3$ (LATP) (Key et al., 2012; Duluard et al., 2013; Morimoto et al., 2013) or when P^{5+} was substituted by Si^{4+} in $Li_{1+x+y}Al_xTi_{2-x}Si_yP_{3-y}O_{12}$ (Fu, 1997; Tan et al., 2012). Conductivity was enhanced significantly to 3×10^{-3} S cm^{-1} for $Li_{1.3}Al_{0.3}Ti_{1.7}(PO_4)_3$ at room temperature.

Due to their excellent Li^+ conductivity and stability in air and water, $LiTi_2(PO_4)_3$-based SEs have been applied to electrochemical energy devices, such as all-solid-state lithium batteries (Yada et al., 2009) and lithium/air secondary batteries (Shimonishi et al., 2011). Besides, NASICON-type SEs can have high electrochemical oxidative voltage. For example, $LiGe_2(PO_4)_3$-based SEs were reported to show high electrochemical oxidative voltage of about 6 V (vs. Li/Li$^+$) (Xu et al., 2007), as shown in **Figure 11**. However, similar to LLTO, $LiTi_2(PO_4)_3$-based SEs are instable toward Li metal, with the reduction of Ti^{4+} to Ti^{3+} (Hartmann et al., 2013).

GLASS-BASED INORGANIC ELECTROLYTES

GLASSY ELECTROLYTES

The glassy electrolytes have attracted much attention mainly due to their several advantages over the crystalline materials: isotropic ionic conduction, no grain-boundary resistance, ease to be fabricated into film, a wide range of compositions, etc. (Ravaine, 1980; Minami, 1987). In addition, the ion conductivity of amorphous glasses is generally higher than that of the corresponding crystalline ones because of their so-called open structure (Tatsumisago, 2004), as shown in **Figure 12**.

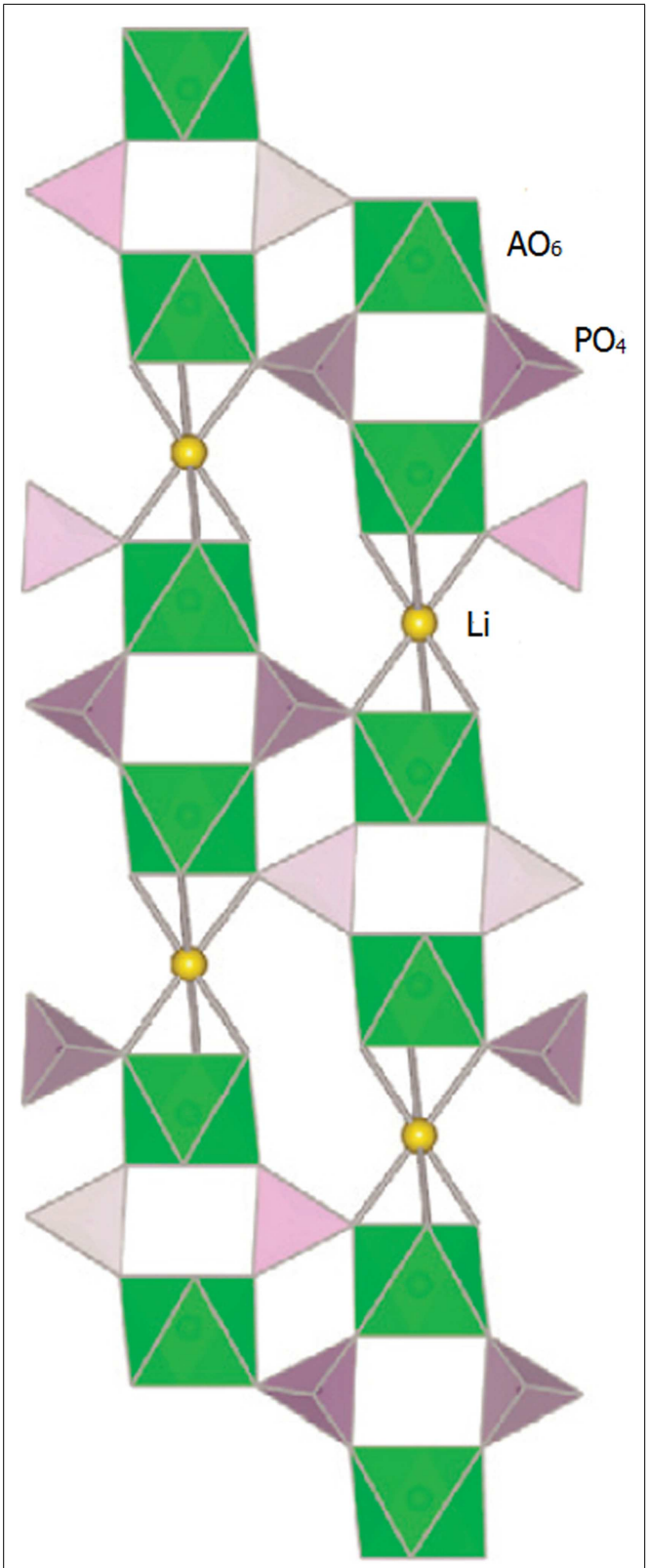

FIGURE 10 | Crystal structure of NASICON. Reproduced with permission of Takada (2009).

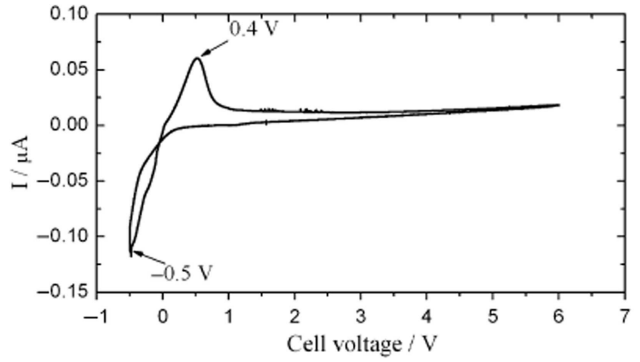

FIGURE 11 | Cyclic voltammogram of $LiGe_2(PO_4)_3$-based SEs. Reproduced with permission of Xu et al. (2007).

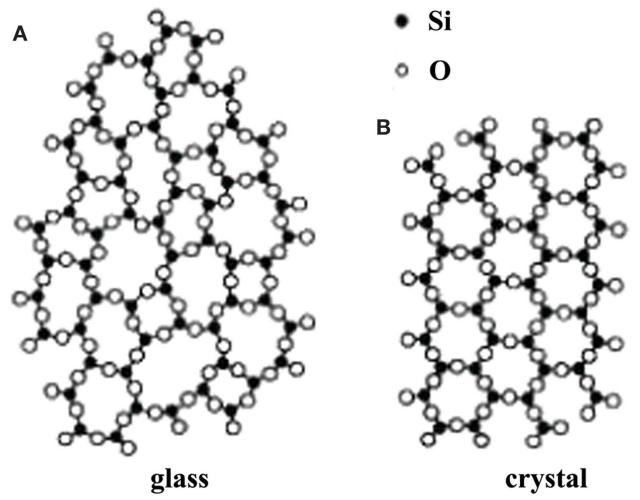

FIGURE 12 | Schematic of structure of SiO_2 (A) glass and (B) crystal.

Generally, lithium ion conducting glasses can be divided into two categories: oxide and sulfide. For most of the oxide glassy electrolytes, the lithium ion conductivity at room temperature is too low to be practical for high energy batteries, normally on the order of $10^{-6} \sim 10^{-8}$ S cm^{-1} (Tatsumisago et al., 1987; Lee et al., 2002). While in sulfide glasses, high lithium ion conductivities of $10^{-3} \sim 10^{-5}$ S cm^{-1} at room temperature can be achieved due to high polarizability of sulfur ions, such as Li_2S–SiS_2 and Li_2S–P_2S_5 (Machida and Shigematsu, 2004; Tatsumisago, 2004; Ohtomo et al., 2013c).

However, these sulfide glass electrolytes can react with ambient moisture and generate H_2S gas (Knauth, 2009). Therefore, handling of sulfide SEs must be done in an inert atmosphere. However, partial substitution of oxygen atoms for sulfur atoms in sulfide electrolytes can be effective in suppressing H_2S gas generation (Ohtomo et al., 2013b). Very recently, Hayashi et al. (2014) reported a composite electrolyte with 90 mol% of $75Li_2S{\cdot}21P_2S_5{\cdot}4P_2O_5$ glass and 10 mol% ZnO via mechanical milling. In the work, partial substitution of P_2O_5 for P_2S_5, as well as the addition of ZnO, decreased the rate of H_2S generation when exposed to air. The conductivity on the other hand decreased with the addition of P_2O_5.

In order to improve the conductivity of glassy electrolytes, several approaches have been proposed. One effective way is to mix two different anion species, so called "mixed anion effect" or "mixed former effect" (Tatsumisago et al., 1987; Raguenet et al., 2012). For instance, the addition of network former or modifier SeO_2 into binary Li_2O–B_2O_3 glassy electrolyte led to the increase in ionic conductivity at room temperature from 1.2×10^{-8} to 8×10^{-7} S cm^{-1} (Lee et al., 2002). The addition of lithium salts such as lithium halides (Ujiie et al., 2012) and lithium ortho-oxosalts (Aotani et al., 1994) is another effective way to enhance the conductivity of glassy electrolytes, because of the increase in lithium concentration and the decrease in activation energy for conduction. For example, the lithium ion conductivity of $67Li_2S{\cdot}33P_2S_5$ glass at room temperature could increase from 10^{-4} S cm^{-1} to 10^{-3} S cm^{-1} by adding 45 mol% of LiI (Mercier et al., 1981).

However, increasing the amount of network modifiers with lithium ions facilitates the crystallization of glass. Thus the glasses with large amount of lithium ions are often prepared by twin-roller rapid quenching (Tatsumisago et al., 1981; Hayashi et al., 2002). This technique allows a cooling rate as high as 10^6 K S^{-1} (Tatsumisago and Hayashi, 2009) to prevent crystallization.

In all-solid-state batteries, the glasses need to be ground into fine powders by mechanical milling techniques (Morimoto et al., 1999) in order to make good contact with the electrodes. Mechanical milling also is a commonly used method to form amorphous materials (Hayashi et al., 2001; Ohtomo et al., 2013a,b). It has two major advantages: the process is very simple and the synthesis can be performed at room temperature.

GLASS–CERAMIC ELECTROLYTES

Glass–ceramic electrolyte can be produced by the crystallization of a precursor glass. The crystallization usually would decrease the ionic conductivity, but the precipitation of a superionic conducting crystal from a precursor glass can enhance ionic conductivity. The grain-boundaries around crystal domains in glass–ceramics are filled with amorphous phases. Thus, glass–ceramic electrolytes usually have lower grain-boundary resistance than polycrystalline systems do (Tatsumisago et al., 2013).

Similar to the case of glassy electrolytes, the glass–ceramics also can be categorized into oxides and sulfides. For glass–ceramic oxides, NASICON-type systems have been studied the most, such as LATP (Fu, 1997b; Kotobuki and Koishi, 2013; Patil et al., 2013) and LAGP (Fu, 1997a; Nikolic et al., 2013; He et al., 2014) glass–ceramics. Their ionic conductivities at room temperature can reach $10^{-3} \sim 10^{-4}$ S cm^{-1}.

Sulfide glass–ceramics can have higher ionic conductivity than that of oxides due to the large ionic radius and high polarizability of sulfur ions than those of oxide ions. For example, the conductivity of Li_2S–P_2S_5 glass–ceramics can reach 10^{-3} S cm^{-1} at room temperature (Tatsumisago et al., 2002).

A superionic crystal with a structure analogous to that of the thio-LISICON phases can be precipitated by mechanical milling Li_2S–P_2S_5 glasses (Hayashi et al., 2003). Very recently, Seino et al.

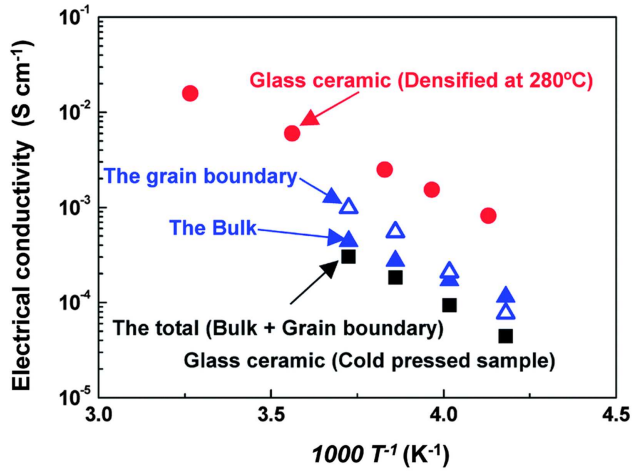

FIGURE 13 | Temperature dependency of the bulk and grain-boundary resistances of the cold-pressed glass–ceramic material. Reproduced with permission of Seino et al. (2014).

(2014) reported a Li_2S–P_2S_5 glass-ceramic conductor that had a very high ionic conductivity of 1.7×10^{-2} S cm^{-1} at room temperature by optimized heat treatment. The optimized conditions of heat treatment reduced the grain-boundary resistance and thus the total conductivity was five-time higher than that previously reported for the Li_2S–P_2S_5 system (Mizuno et al., 2005). As shown in **Figure 13**, it suggested that the densification process increased overall conductivity, not by enhancing ionic conduction in the bulk, but reducing the grain-boundary resistance.

CONCLUDING REMARKS

Solid electrolytes are being viewed as a necessary component for a safe and high-performance lithium battery in future, thereby drawing extensive attention in the field. Many efforts have been made to advance their performance.

Since the high resistance at the electrode/SE interface is one crucial issue for the development of high power all-solid-state lithium batteries, it is of utmost importance to form a favorable contact between electrodes and the electrolyte. Both the achievement of close contact and the increase in contact area are essential (Tatsumisago et al., 2013). Coating of SE thin films on electrode active materials is being explored as an effective route. For instance, Li_2S–GeS_2 sulfide electrolyte thin films with the conductivity of 1.8×10^{-4} S cm^{-1} on $LiCoO_2$ particles were prepared by a pulsed laser deposition (PLD) technique (Ito et al., 2013). From a cross-sectional SEM image, this obtained thin film was dense and attached firmly to the Si substrate. Besides, other techniques, such as preparation of nanocomposites by a ball milling process (Nagao et al., 2012) or utilization of supercooled liquid of glass electrolyte (Kitaura et al., 2011), are documented to be effective in forming an ideal interface between electrodes and the electrolyte.

Regarding the important conductivity, the systems based on sulfur chemistries can show higher ionic conductivities than oxides. For example, in **Table 1**, high ionic conductivities on the order of 10^{-2} S cm^{-1} are achieved in sulfide systems, like thio-LISICON $Li_{10}GeP_2S_{12}$ and Li_2S–P_2S_5 glass–ceramics. On the other hand, sulfides usually are chemically instable and require extra attention to handle. In addition, several effective ways to increasing ionic conductivity have been developed, such as doping, hot isotactic pressing to reduce the grain-boundary resistance, the utilization of "mixed former effect," and the precipitation of superionic crystals from glassy electrolytes.

ACKNOWLEDGMENTS

This work is supported by the "Strategic Priority Research Program" of the Chinese Project Academy of Science, Grant No. XDA01020304, the National Natural Science Foundation of China (Grant No. 51371186), Ningbo 3315 International Team of Advanced Energy Storage Materials, Zhejiang Province Key Science and Technology Innovation Team.

REFERENCES

Abhilash, K. P., Selvin, P. C., Nalini, B., Nithyadharseni, P., and Pillai, B. C. (2013). Investigations on pure and Ag doped lithium lanthanum titanate (LLTO) nanocrystalline ceramic electrolytes for rechargeable lithium-ion batteries. *Ceram. Int.* 39, 947–952. doi:10.1016/j.ceramint.2012.07.011

Allen, J. L., Wolfenstine, J., Rangasamy, E., and Sakamoto, J. (2012). Effect of substitution (Ta, Al, Ga) on the conductivity of $Li_7La_3Zr_2O_{12}$. *J. Power Sources* 206, 315–319. doi:10.1016/j.jpowsour.2012.01.131

Alonso, J., Sanz, J., Santamaria, J., Leon, C., Varez, A., and Fernandez-Diaz, M. (2000). On the location of Li^+ cations in the fast Li-cation conductor $La_{0.5}Li_{0.5}TiO_3$ perovskite. *Angew. Chem. Int. Ed.* 39, 619–621. doi:10.1002/(SICI)1521-3773(20000204)39:3<619::AID-ANIE619>3.0.CO;2-O

Aono, H., Sugimoto, E., Sadaoka, Y., Imanaka, N., and Adachi, G. (1990). Ionic conductivity of solid electrolytes based on lithium titanium phosphate. *J. Electrochem. Soc.* 137, 1023–1027. doi:10.1149/1.2086597

Aotani, N., Iwamoto, K., Takada, K., and Kondo, S. (1994). Synthesis and electrochemical properties of lithium ion conductive glass, Li_3PO_4-Li_2S-SiS_2. *Solid State Ionics* 68, 35–39. doi:10.1016/0167-2738(94)90232-1

Ban, C. W., and Choi, G. M. (2001). The effect of sintering on the grain boundary conductivity of lithium lanthanum titanates. *Solid State Ionics* 140, 285–292. doi:10.1016/S0167-2738(01)00821-9

Bohnke, O. (2008). The fast lithium-ion conducting oxides $Li_{3x}La_{2/3-x}TiO_3$ from fundamentals to application. *Solid State Ionics* 179, 9–15. doi:10.1016/j.ssi.2007.12.022

Bron, P., Johansson, S., Zick, K., Schmedt Auf Der Gunne, J., Dehnen, S., and Roling, B. (2013). $Li_{10}SnP_2S_{12}$: an affordable lithium superionic conductor. *J. Am. Chem. Soc.* 135, 15694–15697. doi:10.1021/ja407393y

Chen, C. H., and Amine, K. (2001). Ionic conductivity, lithium insertion and extraction of lanthanum lithium titanate. *Solid State Ionics* 144, 51–57. doi:10.1016/S0167-2738(01)00884-0

Chen, K., Huang, M., Shen, Y., Lin, Y., and Nan, C. W. (2012). Enhancing ionic conductivity of $Li_{0.35}La_{0.55}TiO_3$ ceramics by introducing $Li_7La_3Zr_2O_{12}$. *Electrochim. Acta* 80, 133–139. doi:10.1016/j.electacta.2012.06.115

Chen, K., Huang, M., Shen, Y., Lin, Y. H., and Nan, C. W. (2013). Improving ionic conductivity of $Li_{0.35}La_{0.55}TiO_3$ ceramics by introducing $Li_7La_3Zr_2O_{12}$ sol into the precursor powder. *Solid State Ionics* 235, 8–13. doi:10.1016/j.ssi.2013.01.007

Cretin, M., and Fabry, P. (1999). Comparative study of lithium ion conductors in the system $Li_{1+x}Al_xA_{2-x}^{IV}(PO_4)^3$ with A^{IV} = Ti or Ge and $0 \leq x \leq 0.7$ for use as Li^+ sensitive membranes. *J. Eur. Ceram. Soc.* 19, 2931–2940. doi:10.1016/S0955-2219(99)00055-2

Duluard, S., Paillassa, A., Puech, L., Vinatier, P., Turq, V., Rozier, P., et al. (2013). Lithium conducting solid electrolyte $Li_{1.3}Al_{0.3}Ti_{1.7}(PO_4)_3$ obtained via solution chemistry. *J. Eur. Ceram. Soc.* 33, 1145–1153. doi:10.1016/j.jeurceramsoc.2012.08.005

Dumon, A., Huang, M., Shen, Y., and Nan, C. W. (2013). High Li ion conductivity in strontium doped $Li_7La_3Zr_2O_{12}$ garnet. *Solid State Ionics* 243, 36–41. doi:10.1016/j.ssi.2013.04.016

Düvel, A., Kuhn, A., Robben, L., Wilkening, M., and Heitjans, P. (2012). Mechanosynthesis of solid electrolytes: preparation, characterization, and Li ion transport

properties of garnet-type Al-doped $Li_7La_3Zr_2O_{12}$ crystallizing with cubic symmetry. *J. Phys. Chem. C* 116, 15192–15202. doi:10.1021/jp301193r

Fergus, J. W. (2010). Ceramic and polymeric solid electrolytes for lithium-ion batteries. *J. Power Sources* 195, 4554–4569. doi:10.1016/j.jpowsour.2010.01.076

Fu, J. (1997). Fast Li^+ ion conduction in Li_2O-Al_2O_3-TiO_2-SiO_2-P_2O_5 glass-ceramics. *J. Am. Ceram. Soc.* 80, 1901–1903. doi:10.1111/j.1151-2916.1997.tb03070.x

Fu, J. (1997a). Fast Li^+ ion conducting glass-ceramics in the system Li_2O-Al_2O_3-GeO_2-P_2O_5. *Solid State Ionics* 104, 191–194. doi:10.1016/S0167-2738(97)00434-7

Fu, J. (1997b). Superionic conductivity of glass-ceramics in the system Li_2O-Al_2O_3-TiO_2-P_2O_5. *Solid State Ionics* 96, 195–200. doi:10.1016/S0167-2738(97)00018-0

Gao, X., Fisher, C. A. J., Kimura, T., Ikuhara, Y. H., Moriwake, H., Kuwabara, A., et al. (2013). Lithium atom and A-site vacancy distributions in lanthanum lithium titanate. *Chem. Mater.* 25, 1607–1614. doi:10.1021/cm3041357

Geiger, C. A., Alekseev, E., Lazic, B., Fisch, M., Armbruster, T., Langner, R., et al. (2011). Crystal chemistry and stability of "$Li_7La_3Zr_2O_{12}$" garnet: a fast lithium-ion conductor. *Inorg. Chem.* 50, 1089–1097. doi:10.1021/ic101914e

Goodenough, J. B., and Kim, Y. (2009). Challenges for rechargeable Li batteries. *Chem. Mater.* 22, 587–603. doi:10.1021/cm901452z

Hartmann, P., Leichtweiss, T., Busche, M. R., Schneider, M., Reich, M., Sann, J., et al. (2013). Degradation of NASICON-type materials in contact with lithium metal: formation of mixed conducting interphases (MCI) on solid electrolytes. *J. Phys. Chem. C* 117, 21064–21074. doi:10.1021/jp4051275

Hayashi, A., Hama, S., Minami, T., and Tatsumisago, M. (2003). Formation of superionic crystals from mechanically milled Li_2S-P_2S_5 glasses. *Electrochem. Commun.* 5, 111–114. doi:10.1016/S1388-2481(02)00555-6

Hayashi, A., Hama, S., Morimoto, H., Tatsumisago, M., and Minami, T. (2001). Preparation of Li_2S-P_2S_5 amorphous solid electrolytes by mechanical milling. *J. Am. Ceram. Soc.* 84, 477–479. doi:10.1111/j.1151-2916.2001.tb00685.x

Hayashi, A., Komiya, R., Tatsumisago, M., and Minami, T. (2002). Characterization of Li_2S-SiS_2-Li_3MO_3 (M=B, Al, Ga and In) oxysulfide glasses and their application to solid state lithium secondary batteries. *Solid State Ionics* 15, 285–290. doi:10.1016/S0167-2738(02)00313-2

Hayashi, A., Muramatsu, H., Ohtomo, T., Hama, S., and Tatsumisago, M. (2014). Improved chemical stability and cyclability in Li_2S-P_2S_5-P_2O_5-ZnO composite electrolytes for all-solid-state rechargeable lithium batteries. *J. Alloy. Compd.* 591, 247–250. doi:10.1016/j.jallcom.2013.12.191

Hayashi, A., Noi, K., Sakuda, A., and Tatsumisago, M. (2012). Superionic glass-ceramic electrolytes for room-temperature rechargeable sodium batteries. *Nat. Commun.* 3, 856–860. doi:10.1038/ncomms1843

He, K., Zu, C., Wang, Y., Han, B., Yin, X., Zhao, H., et al. (2014). Stability of lithium ion conductor NASICON structure glass ceramic in acid and alkaline aqueous solution. *Solid State Ionics* 254, 78–81. doi:10.1016/j.ssi.2013.11.011

Hong, H. Y. P. (1976). Crystal structures and crystal chemistry in the system $Na_{1+x}Zr_2Si_xP_{3-x}O_{12}$. *Mater. Res. Bull.* 11, 173–182. doi:10.1016/0025-5408(76)90073-8

Hong, H. Y.-P. (1978). Crystal structure and ionic conductivity of $Li_{14}Zn(GeO_4)_4$ and other new Li^+ superionic conductors. *Mater. Res. Bull.* 13, 117–124. doi:10.1016/0025-5408(78)90075-2

Inaguma, Y., and Nakashima, M. (2013). A rechargeable lithium-air battery using a lithium ion-conducting lanthanum lithium titanate ceramics as an electrolyte separator. *J. Power Sources* 228, 250–255. doi:10.1016/j.jpowsour.2012.11.098

Ishiguro, K., Nakata, Y., Matsui, M., Uechi, I., Takeda, Y., Yamamoto, O., et al. (2013). Stability of Nb-doped cubic $Li_7La_3Zr_2O_{12}$ with lithium metal. *J. Electrochem. Soc.* 160, A1690–A1693. doi:10.1039/c2cp40634a

Ito, Y., Sakuda, A., Ohtomo, T., Hayashi, A., and Tatsumisago, M. (2013). Preparation of Li_2S-GeS_2 solid electrolyte thin films using pulsed laser deposition. *Solid State Ionics* 236, 1–4. doi:10.1016/j.ssi.2013.01.014

Jin, Y., and McGinn, P. J. (2013a). Bulk solid state rechargeable lithium ion battery fabrication with Al-doped $Li_7La_3Zr_2O_{12}$ electrolyte and $Cu_{0.1}V_2O_5$ cathode. *Electrochim. Acta* 89, 407–412. doi:10.1016/j.electacta.2012.11.059

Jin, Y., and McGinn, P. J. (2013b). $Li_7La_3Zr_2O_{12}$ electrolyte stability in air and fabrication of a Li/$Li_7La_3Zr_2O_{12}$/$Cu_{0.1}V_2O_5$ solid-state battery. *J. Power Sources* 239, 326–331. doi:10.1016/j.jpowsour.2013.03.155

Kamaya, N., Homma, K., Yamakawa, Y., Hirayama, M., Kanno, R., Yonemura, M., et al. (2011). A lithium superionic conductor. *Nat. Mater.* 10, 682–686. doi:10.1038/nmat3066

Kanno, R., Hata, T., Kawamoto, Y., and Irie, M. (2000). Synthesis of a new lithium ionic conductor, thio-LISICON-lithium germanium sulfide system. *Solid State Ionics* 130, 97–104. doi:10.1016/S0167-2738(00)00277-0

Kanno, R., and Murayama, M. (2001). Lithium ionic conductor thio-LISICON: the Li_2S-GeS_2-P_2S_5 system. *J. Electrochem. Soc.* 148, A742–A746. doi:10.1149/1.1379028

Key, B., Schroeder, D. J., Ingram, B. J., and Vaughey, J. T. (2012). Solution-based synthesis and characterization of lithium-ion conducting phosphate ceramics for lithium metal batteries. *Chem. Mater.* 24, 287–293. doi:10.1021/cm202773d

Kitaura, H., Hayashi, A., Ohtomo, T., Hama, S., and Tatsumisago, M. (2011). Fabrication of electrode-electrolyte interfaces in all-solid-state rechargeable lithium batteries by using a supercooled liquid state of the glassy electrolytes. *J. Mater. Chem.* 21, 118. doi:10.1039/c0jm01090a

Knauth, P. (2009). Inorganic solid Li ion conductors: an overview. *Solid State Ionics* 180, 911–916. doi:10.1016/j.ssi.2009.03.022

Kokal, I., Somer, M., Notten, P. H. L., and Hintzen, H. T. (2011). Sol-gel synthesis and lithium ion conductivity of $Li_7La_3Zr_2O_{12}$ with garnet-related type structure. *Solid State Ionics* 185, 42–46. doi:10.1016/j.ssi.2011.01.002

Kotobuki, M. (2012). The current situation and problems of rechargeable lithium ion batteries. *Open Electrochem. J.* 4, 28–35. doi:10.2174/1876505X01204010028

Kotobuki, M., and Koishi, M. (2013). Preparation of $Li_{1.5}Al_{1.5}(PO_4)_3$ solid electrolyte via a sol-gel route using various Al sources. *Ceram. Int.* 39, 4645–4649. doi:10.1016/j.ceramint.2012.10.206

Lee, C. H., Joo, K. H., Kim, J. H., Woo, S. G., Sohn, H. J., Kang, T., et al. (2002). Characterizations of a new lithium ion conducting Li_2O-SeO_2-B_2O_3 glass electrolyte. *Solid State Ionics* 149, 59–65. doi:10.1016/S0167-2738(02)00137-6

Machida, N., and Shigematsu, T. (2004). An all-solid-state lithium battery with sulfur as positive electrode materials. *Chem. Lett.* 33, 376–377. doi:10.1246/cl.2004.376

Mei, A., Wang, X. L., Lan, J. L., Feng, Y. C., Geng, H. X., Lin, Y. H., et al. (2010). Role of amorphous boundary layer in enhancing ionic conductivity of lithium-lanthanum-titanate electrolyte. *Electrochim. Acta* 55, 2958–2963. doi:10.1016/j.electacta.2010.01.036

Mercier, R., Malugani, J. P., Fahys, B., and Robert, G. (1981). Superionic conduction in Li_2S-P_2S_5-LiI-glasses. *Solid State Ionics* 5, 663–666. doi:10.1016/0167-2738(81)90341-6

Minami, T. (1987). Recent progress in superionic conducting glasses. *J. Non Cryst. Solids* 95–96(Part 1), 107–118. doi:10.1016/S0022-3093(87)80103-5

Mizuno, F., Hayashi, A., Tadanaga, K., and Tatsumisago, M. (2005). New, highly ion-conductive crystals precipitated from Li_2S-P_2S_5 glasses. *Adv. Mater.* 17, 918–921. doi:10.1002/adma.200401286

Morata-Orrantia, A., García-Martí, G., and Alario-Franco, M. (2003). Optimization of lithium conductivity in La/Li titanates. *Chem. Mater.* 15, 3991–3995. doi:10.1021/cm0300563

Morimoto, H., Awano, H., Terashima, J., Shindo, Y., Nakanishi, S., Ito, N., et al. (2013). Preparation of lithium ion conducting solid electrolyte of NASICON-type $Li_{1+x}Al_xTi_{2-x}(PO_4)_3$ (x 0.3) obtained by using the mechanochemical method and its application as surface modification materials of $LiCoO_2$ cathode for lithium cell. *J. Power Sources* 240, 636–643. doi:10.1016/j.jpowsour.2013.05.039

Morimoto, H., Yamashita, H., Tatsumisago, M., and Minami, T. (1999). Mechanochemical synthesis of new amorphous materials of $60Li_2S{\cdot}40SiS_2$ with high lithium ion conductivity. *J. Am. Ceram. Soc.* 82, 1352–1354. doi:10.1111/j.1151-2916.1999.tb01923.x

Murugan, R., Thangadurai, V., and Weppner, W. (2007). Fast lithium ion conduction in garnet-type $Li_7La_3Zr_2O_{12}$. *Angew. Chem. Int. Ed.* 46, 7778–7781. doi:10.1002/anie.200701144

Nagao, M., Hayashi, A., and Tatsumisago, M. (2012). High-capacity Li_2S-nanocarbon composite electrode for all-solid-state rechargeable lithium batteries. *J. Mater. Chem.* 22, 10015–10020. doi:10.1039/c2jm16802b

Narayanan, S., Ramezanipour, F., and Thangadurai, V. (2012). Enhancing Li ion conductivity of garnet-type $Li_5La_3Nb_2O_{12}$ by Y- and Li-codoping: synthesis, structure, chemical stability, and transport properties. *J. Phys. Chem. C* 116, 20154–20162. doi:10.1021/jp304737x

Nikolić, J. D., Smiljanjić, S. V., Matijašević, S. D., Živanović, V. D., Tošić, M. B., Grujić, S. R. et al. (2013). Preparation of glass-ceramic in Li_2O-Al_2O_3-GeO_2-P_2O_5 system. *Process. Appl. Ceram.* 7, 147–151. doi:10.2298/PAC1304147N

Ohta, N., Takada, K., Sakaguchi, I., Zhang, L., Ma, R., Fukuda, K., et al. (2007). $LiNbO_3$-coated $LiCoO_2$ as cathode material for all solid-state lithium secondary

batteries. *Electrochem. Commun.* 9, 1486–1490. doi:10.1016/j.elecom.2007.02.008

Ohta, N., Takada, K., Zhang, L., Ma, R., Osada, M., and Sasaki, T. (2006). Enhancement of the high-rate capability of solid-state lithium batteries by nanoscale interfacial modification. *Adv. Mater.* 18, 2226–2229. doi:10.1002/adma.200502604

Ohta, S., Kobayashi, T., Seki, J., and Asaoka, T. (2012). Electrochemical performance of an all-solid-state lithium ion battery with garnet-type oxide electrolyte. *J. Power Sources* 202, 332–335. doi:10.1016/j.jpowsour.2011.10.064

Ohtomo, T., Hayashi, A., Tatsumisago, M., and Kawamoto, K. (2013a). All-solid-state batteries with Li_2O-Li_2S-P_2S_5 glass electrolytes synthesized by two-step mechanical milling. *J. Solid State Electrochem.* 17, 2551–2557. doi:10.1007/s10008-013-2149-5

Ohtomo, T., Hayashi, A., Tatsumisago, M., and Kawamoto, K. (2013b). Characteristics of the Li_2O-Li_2S-P_2S_5 glasses synthesized by the two-step mechanical milling. *J. Non Cryst. Solids* 364, 57–61. doi:10.1016/j.jnoncrysol.2012.12.044

Ohtomo, T., Hayashi, A., Tatsumisago, M., Tsuchida, Y., Hama, S., and Kawamoto, K. (2013c). All-solid-state lithium secondary batteries using the $75Li_2S{\cdot}25P_2S_5$ glass and the $70Li_2S{\cdot}30P_2S_5$ glass-ceramic as solid electrolytes. *J. Power Sources* 233, 231–235. doi:10.1016/j.jpowsour.2013.01.090

Patil, V., Patil, A., Yoon, S. J., and Choi, J. W. (2013). Structural and electrical properties of NASICON type solid electrolyte nanoscaled glass-ceramic powder by mechanical milling for thin film batteries. *J. Nanosci. Nanotech.* 13, 3665–3668. doi:10.1166/jnn.2013.7240

Qian, D., Xu, B., Cho, H. M., Hatsukade, T., Carroll, K. J., and Meng, Y. S. (2012). Lithium lanthanum titanium oxides: a fast ionic conductive coating for lithium-ion battery cathodes. *Chem. Mater.* 24, 2744–2751. doi:10.1021/cm300929r

Quartarone, E., and Mustarelli, P. (2011). Electrolytes for solid-state lithium rechargeable batteries: recent advances and perspectives. *Chem. Soc. Rev.* 40, 2525–2540. doi:10.1039/c0cs00081g

Raguenet, B., Tricot, G., Silly, G., Ribes, M., and Pradel, A. (2012). The mixed glass former effect in twin-roller quenched lithium borophosphate glasses. *Solid State Ionics* 208, 25–30. doi:10.1016/j.ssi.2011.11.034

Ravaine, D. (1980). Glasses as solid electrolytes. *J. Non Cryst. Solids* 38–39(Part 1), 353–358. doi:10.1016/0022-3093(80)90444-5

Robertson, A. D., West, A. R., and Ritchie, A. G. (1997). Review of crystalline lithium-ion conductors suitable for high temperature battery applications. *Solid State Ionics* 104, 1–11. doi:10.1016/S0167-2738(97)00429-3

Sahu, G., Lin, Z., Li, J. C., Liu, Z. C., Dudney, N., and Liang, C. D. (2014). Air-stable, high-conduction solid electrolytes of arsenic-substituted Li_4SnS_4. *Energy Environ. Sci.* 7, 1053–1058. doi:10.1039/c3ee43357a

Sakuda, A., Hayashi, A., Ohtomo, T., Hama, S., and Tatsumisago, M. (2011). All-solid-state lithium secondary batteries using $LiCoO_2$ particles with pulsed laser deposition coatings of Li_2S-P_2S_5 solid electrolytes. *J. Power Sources* 196, 6735–6741. doi:10.1021/am302164e

Seino, Y., Ota, T., Takada, K., Hayashi, A., and Tatsumisago, M. (2014). A sulphide lithium super ion conductor is superior to liquid ion conductors for use in rechargeable batteries. *Energy Environ. Sci.* 7, 627–631. doi:10.1039/c3ee41655k

Shimonishi, Y., Zhang, T., Imanishi, N., Im, D., Lee, D. J., Hirano, A., et al. (2011). A study on lithium/air secondary batteries – stability of the NASICON-type lithium ion conducting solid electrolyte in alkaline aqueous solutions. *J. Power Sources* 196, 5128–5132. doi:10.1016/j.jpowsour.2011.02.023

Stramare, S., Thangadurai, V., and Weppner, W. (2003). Lithium lanthanum titanates: a review. *Chem. Mater.* 15, 3974–3990. doi:10.1088/0953-8984/22/40/404203

Takada, K. (2009). Electrolytes: solid oxide. *Enc. Electrochem. Power Sources* 5, 328–336. doi:10.1016/B978-044452745-5.00211-2

Tan, G. Q., Wu, F., Li, L., Liu, Y. D., and Chen, R. J. (2012). Magnetron sputtering preparation of nitrogen-incorporated lithium-aluminum-titanium phosphate based thin film electrolytes for all-solid-state lithium ion batteries. *J. Phys. Chem. C* 116, 3817–3826. doi:10.1021/jp207120s

Tatsumisago, M. (2004). Glassy materials based on Li_2S for all-solid-state lithium secondary batteries. *Solid State Ionics* 175, 13–18. doi:10.1016/j.ssi.2004.09.012

Tatsumisago, M., Hachida, N., and Minami, T. (1987). Mixed anion effect in conductivity of rapidly quenched Li_4SiO_4-Li_3BO_3 glasses. *Yogyo Kyokaishi.* 95, 197–201. doi:10.2109/jcersj1950.95.1098_197

Tatsumisago, M., Hama, S., Hayashi, A., Morimoto, H., and Minami, T. (2002). New lithium ion conducting glass-ceramics prepared from mechanochemical Li_2S-P_2S_5 glasses. *Solid State Ionics* 15, 635–640. doi:10.1016/S0167-2738(02)00509-X

Tatsumisago, M., and Hayashi, A. (2009). "Secondary batteries-lithium rechargeable systems – electrolytes: Glass," in *Encyclopedia of Electrochemical Power Source*, ed. J. Garche, et al. (Amsterdam: Elsevier B.V.), 138–144.

Tatsumisago, M., Minami, T., and Tanaka, M. (1981). Rapid thermal-image furnace for glass preparation. *J. Am. Ceram. Soc.* 64, C–97–C–98. doi:10.1111/j.1151-2916.1981.tb09886.x

Tatsumisago, M., Nagao, M., and Hayashi, A. (2013). Recent development of sulfide solid electrolytes and interfacial modification for all-solid-state rechargeable lithium batteries. *J. Asian Ceram. Soc.* 1, 17–25. doi:10.1016/j.jascer.2013.03.005

Teranishi, T., Yamamoto, M., Hayashi, H., and Kishimoto, A. (2013). Lithium ion conductivity of Nd-doped (Li, La)TiO_3 ceramics. *Solid State Ionics* 243, 18–21. doi:10.1016/j.ssi.2013.04.014

Thangadurai, V., and Weppner, W. (2005a). $Li_6ALa_2Nb_2O_{12}$ (A=Ca, Sr, Ba): a new class of fast lithium ion conductors with garnet-like structure. *J. Am. Ceram. Soc.* 88, 411–418. doi:10.1111/j.1551-2916.2005.00060.x

Thangadurai, V., and Weppner, W. (2005b). $Li_6ALa_2Ta_2O_{12}$(A=Sr, Ba):novel garnet-like oxides for fast lithium ion conduction. *Adv. Funct. Mater.* 15, 107–112. doi:10.1039/c4cs00020j

Thangadurai, V., and Weppner, W. (2006a). Effect of sintering on the ionic conductivity of garnet-related structure $Li_5La_3Nb_2O_{12}$ and In- and K-doped $Li_5La_3Nb_2O_{12}$. *J. Solid State Chem.* 179, 974–984. doi:10.1016/j.jssc.2005.12.025

Thangadurai, V., and Weppner, W. (2006b). Recent progress in solid oxide and lithium ion conducting electrolytes research. *Ionics* 12, 81–92. doi:10.1007/s11581-006-0013-7

Tietz, F., Wegener, T., Gerhards, M. T., Giarola, M., and Mariotto, G. (2013). Synthesis and Raman micro-spectroscopy investigation of $Li_7La_3Zr_2O_{12}$. *Solid State Ionics* 230, 77–82. doi:10.1016/j.ssi.2012.10.021

Ujiie, S., Hayashi, A., and Tatsumisago, M. (2012). Structure, ionic conductivity and electrochemical stability of Li_2S-P_2S_5-LiI glass and glass-ceramic electrolytes. *Solid State Ionics* 211, 42–45. doi:10.1016/j.ssi.2012.01.017

Vidal, K., Ortega-San-Martín, L., Larrañaga, A., Merino, R. I., Orera, A., and Arriortua, M. I. (2014). Effects of synthesis conditions on the structural, stability and ion conducting properties of $Li_{0.30}(La_{0.50}Ln_{0.50})_{0.567}TiO_3$ (Ln=La, Pr, Nd) solid electrolytes for rechargeable lithium batteries. *Ceram. Int.* 40, 8761–8768. doi:10.1016/j.ceramint.2014.01.097

Xu, X. X., Wen, Z. Y., Wu, X. W., Yang, X. L., and Gu, Z. H. (2007). Lithium ion-conducting glass-ceramics of $Li_{1.5}Al_{0.5}Ge_{1.5}(PO_4)_3$-$xLi_2O$ (x=0.0-0.20) with good electrical and electrochemical properties. *J. Am. Ceram. Soc.* 90, 2802–2806. doi:10.1111/j.1551-2916.2007.01827.x

Yada, C., Iriyama, Y., Abe, T., Kikuchi, K., and Ogumi, Z. (2009). A novel all-solid-state thin-film-type lithium-ion battery with in situ prepared positive and negative electrode materials. *Electrochem. Commun.* 11, 413–416. doi:10.1016/j.elecom.2008.12.004

Yamauchi, A., Sakuda, A., Hayashi, A., and Tatsumisago, M. (2013). Preparation and ionic conductivities of $(100\text{-}x)(0.75Li_2S{\cdot}0.25P_2S_5){\cdot}xLiBH_4$ glass electrolytes. *J. Power Sources* 244, 707–710. doi:10.1016/j.jpowsour.2012.12.001

Zheng, Z. S., Zhang, Z. T., Tang, Z. L., and Shen, W. C. (2003). Lithium inorganic solid electrolytes. *Prog. Chem.* 15, 101–106. doi:10.3321/j.issn:1005-281X.2003.02.003

Conflict of Interest Statement: The authors declare that the research was conducted in the absence of any commercial or financial relationships that could be construed as a potential conflict of interest.

Received: 16 April 2014; accepted: 11 June 2014; published online: 27 June 2014.
Citation: Cao C, Li Z-B, Wang X-L, Zhao X-B and Han W-Q (2014) Recent advances in inorganic solid electrolytes for lithium batteries. Front. Energy Res. ***2****:25. doi: 10.3389/fenrg.2014.00025*
This article was submitted to Energy Storage, a section of the journal Frontiers in Energy Research.